TISSUE ENGINEERING: Part A
Volume 16, Number 7, 2010

DOI: 10.1089/ten.tea.2009.0670

Oxygen-Controlled Three-Dimensional Cultures to Analyze Tumor Angiogenesis

Scott S. Verbridge, Ph.D.,[1,*] Nak Won Choi, Ph.D.,[2,*] Ying Zheng, Ph.D.,[2] Daniel J. Brooks, M.S.,[1] Abraham D. Stroock, Ph.D.,[2] and Claudia Fischbach, Ph.D.[1]

Tumor angiogenesis is controlled by the integrated action of physicochemical and biological cues; however, the individual contributions of these cues are not well understood. We have designed alginate-based microscale tumor models to define the distinct importance of oxygen concentration, culture dimensionality, and cell–extracellular matrix interactions on the angiogenic capability of oral squamous cell carcinoma, and have verified the relevance of our findings with U87 glioblastoma cells. Our results revealed qualitative differences in the microenvironmental regulation of vascular endothelial growth factor (VEGF) and interleukin-8 (IL-8) secretion in three-dimensional (3D) culture. Specifically, IL-8 secretion was highest under ambient conditions, whereas VEGF secretion was highest in hypoxic cultures. Additionally, 3D integrin engagement by RGD-modified alginate matrices increased IL-8 secretion independently of oxygen, whereas VEGF secretion was only moderately affected by cell–extracellular matrix interactions. Using two-dimensional migration assays and a new 3D tumor angiogenesis model, we demonstrated that the resulting angiogenic signaling promotes tumor angiogenesis by increasing endothelial cell migration and invasion. Collectively, tissue-engineered tumor models improve our understanding of tumor angiogenesis, which may ultimately advance anticancer therapies.

Introduction

The capacity of tumor cells to drive angiogenesis—the formation of new blood vessels—is a hallmark of cancer. This process is typically regulated by spatiotemporal changes in tissue oxygen (O_2) levels.[1–3] Initially, tumors grow as an avascular mass until they reach a critical size where the center of the tumor becomes depleted of O_2, or hypoxic, due to limitations in O_2 diffusion. Consequently, tumor cells activate intracellular signaling pathways that induce tumor angiogenesis, a process that enables tumor growth and metastasis.[4,5]

Hypoxia-mediated upregulation of vascular endothelial growth factor (VEGF) is considered paramount in activating the angiogenic switch[2,6–8]; however, microenvironmental cues may also play an important role in this process and may regulate angiogenic factor expression independent of changes in tissue O_2 levels.[9,10] For example, culture dimensionality and cell–extracellular matrix (ECM) interactions regulate expression of pro-angiogenic factors such as basic fibroblast growth factor and interleukin-8 (IL-8),[11,12] and the resulting multifactorial signaling may be implicated in the limited clinical success of VEGF-inhibiting therapies.[7,13–15]

Tumor cell response to hypoxia is traditionally studied in two-dimensional (2D) cell culture, with human tumor biopsies, or in animal models.[3,16–19] However, these systems fail to recapitulate physiologically relevant, spatiotemporal variations in O_2 concentration[9,11,20] or to define experimental parameters quantitatively. Three-dimensional (3D) tumor models offer the potential to recreate cell–microenvironment interactions that recapitulate human tumor behavior.[11,12,21,22] Nevertheless, O_2 levels in conventional 3D culture systems are typically uncontrolled and heterogeneous as a result of cellular consumption and size-dependent limitations in O_2-diffusion.[23–25]

The goal of this study was to investigate the individual contributions of O_2 concentration, culture dimensionality, cell–ECM interactions, and the coupling of these effects on tumor angiogenesis. We engineered microfabricated 3D tumor models based on measured O_2 consumption rates and mathematical modeling of intratumor O_2 distributions. These models allowed for the control of intraculture O_2 by incubation under ambient and hypoxic conditions, and were prepared from nonmodified and RGD-modified alginate to prevent and enable 3D integrin engagement, respectively. Comparison of VEGF and IL-8 secretion in these systems with conventional monolayer cultures allowed us to isolate the distinct effects of O_2 status, culture dimensionality, and cell–ECM interactions on the angiogenic potential of oral squamous cell carcinoma (OSCC-3) (Fig. 1a). We further confirmed the relevance of our findings with U87 glioblastoma

[1]Department of Biomedical Engineering and [2]School of Chemical and Biomolecular Engineering, Cornell University, Ithaca, New York.
*These authors contributed equally to this work.

cells. With this distinction made, we designed a 3D model of invasion angiogenesis that has the potential to define the resulting effects on endothelial cell behavior under pathologically relevant conditions *in vitro*.

Materials and Methods

Three-dimensional alginate-based tumor models

Alginate hydrogels (4% [w/v]) were used for 3D cell culture of human OSCC-3 (gift from Peter Polverini, University of Michigan), an oral cancer cell line, and human U87 glioblastoma cells (ATCC). Cylindrical calcium alginate disks (200 μm thick and 4 mm in diameter) were made by (1) suspending cells in alginate (Protanal LF; FMC Biopolymer, Philadelphia, PA; dissolved in serum-free Dulbecco's modified Eagle's medium) at a concentration of 20×10^6 cells/mL, (2) casting in a machined Plexiglass mold, and (3) cross-linking with 60 mM $CaCl_2$. Cross-linked, cell-seeded disks were removed from the mold, and cultured in 24-well plates (one disk per well) on an orbital shaker (Fig. 1b). The medium was Dulbecco's modified Eagle's medium with 10% [v/v] fetal bovine serum (Lonza, Inc., Walkersville, MD) and 1% penicillin/streptomycin (PS), and culture was performed at 37°C, 5% CO_2, and either hypoxic (1%) or ambient ($18\pm1\%$) O_2, in a controlled atmosphere incubator (Thermo Fisher Scientific, Inc., Waltham, MA). For analysis of cell–ECM interactions, alginate was covalently modified with RGD-peptides as previously described.[12,26] Growth-arrested OSCC-3 were prepared by incubating cells with 1 μg/mL mitomycin-C for 2 h before mixing with alginate.[27]

Measurement of O_2 consumption and finite element modeling

OSCC-3 O_2 consumption was measured from four cell-seeded 200-μm-thick alginate disks submerged in 2 mL medium in a sealed glass chamber (Agilent Technologies, Inc., Santa Clara, CA), and kept stirring at 37°C. The medium was initially equilibrated at ambient O_2 and 5% CO_2, and reduction in O_2 level due to cellular consumption was measured with a dissolved O_2 meter (Innovative Instruments, Inc., Tampa, FL). Measurements were taken at minute intervals for 30 min. Consumption rate was calculated from a linear fit to the O_2 level versus time (Fig. 2a, calibration in the absence of cells verified no reduction in O_2 level with time; Supplemental Fig. S1, available online at www.liebertonline.com/ten). We treated consumption kinetics as zeroth order in the range measured (from 13% to 5% O_2). To calculate O_2 consumption per cell DNA, content of the suspended disks was measured using Quant-iT™ PicoGreen® dsDNA reagent (Invitrogen Co., Carlsbad, CA) and converted to cell number (based on a determined conversion factor of 15.1 pg DNA/OSCC-3 cell). Using this consumption rate ($R=5.4\times10^{-17}$ mol/s-cell), a reported O_2 diffusion constant (D) for water,[28] a cell seeding density of 20×10^6 cell/mL, and assumption of proliferation by a factor of three, the cross-sectional O_2 profile in disks of 200, 500, and 1000 μm thickness (after 3 days of culture) was computed by solution of the steady-state diffusion–reaction equation $D\nabla^2 c_{O_2}=\rho_{cell}R_{O_2,cell}$. This continuum approach was appropriate for the relevant values of ρ_{cell}, D, and $R_{O_2,cell}$, and for the typical radius of the cells (~8 μm); the O_2 gradients associated with individual cells were small compared to the global gradient in the matrix (see Supplemental Material, available online at www.liebertonline.com), confirming the absence of localized zones of O_2 depletion that might not be captured by the global model. The solution was obtained with finite element modeling, implemented with Comsol Multiphysics (Comsol, Inc., Burlington, MA), assuming a fixed boundary concentration at 17% O_2. To avoid mass transfer limitations for delivery of O_2 to the boundaries of the disks, disks were cultured on an orbital shaker.

Histological analysis

Alginate disks were incubated with hypoxyprobe (HPI, Inc., Burlington, MA) for 90 min before harvesting, and prepared for paraffin embedding and cross sectioning. Hematoxylin and eosin–stained sections were imaged to determine cellularity. Hypoxyprobe immunostaining was performed to identify regions of hypoxia. Bright-field images were taken on an inverted microscope (Axio Observer; Carl Zeiss, Inc., Thornwood, NY).

Analysis of angiogenic factor secretion

To measure angiogenic factor secretion, tumor models were transferred to a fresh medium before sample collection. After 24 h, the conditioned medium was collected, and soluble VEGF and IL-8 content was analyzed by ELISA (R&D Systems, Minneapolis, MN). Alginate disks were dissolved using ethylenediaminetetraacetic acid and released cells were lysed in Caron's buffer. DNA content was measured using Quant-iT PicoGreen dsDNA reagent (Invitrogen Co.), and used to normalize VEGF and IL-8 secretion. Media from monolayer cultures were harvested at day 2 to ensure that the rapidly proliferating tumor cells had not formed 3D aggregates. Three-dimensional cultures were harvested at day 3.

Transwell assay

Tissue culture inserts (polycarbonate membranes, 8 μm pores) were coated with collagen (22 μg/mL) and seeded with 10^4 cell/well human umbilical vein endothelial cells (HUVECs; Lonza, Inc.). Control (HUVEC medium), tumor-conditioned (medium collected from the 3D alginate culture of OSCC-3, concentrated, and then reconstituted in the HUVEC medium), or neutralized tumor-conditioned medium treated with IL-8 antibody was placed below the insert, and cells allowed to migrate toward the underlying medium for 24 h. After fixation and removal of nonmigrated cells, migrated cells were stained with 4′,6-diamidino-2-phenylindole, imaged, and counted with ImageJ (rsbweb.nih.gov/ij).

Three-dimensional collagen-based tumor angiogenesis models

Collagen-based invasion models were fabricated in a microwell format (Fig. 1c), for ease of handling. Collagen was chosen as a scaffold material that can be both invaded and remodeled by endothelial cells. Square collagen scaffolds (2.5×2.5 mm; 90 and 400 μm thick) were made by (1) isolating and mixing concentrated rat-tail collagen at 0, 5×10^6, or 20×10^6 cell/mL OSCC-3 to yield 0.675% collagen gels, (2) casting in a microfabricated poly(dimethylsiloxane) (PDMS) mold that was precoated sequentially with 1% [v/v] poly-

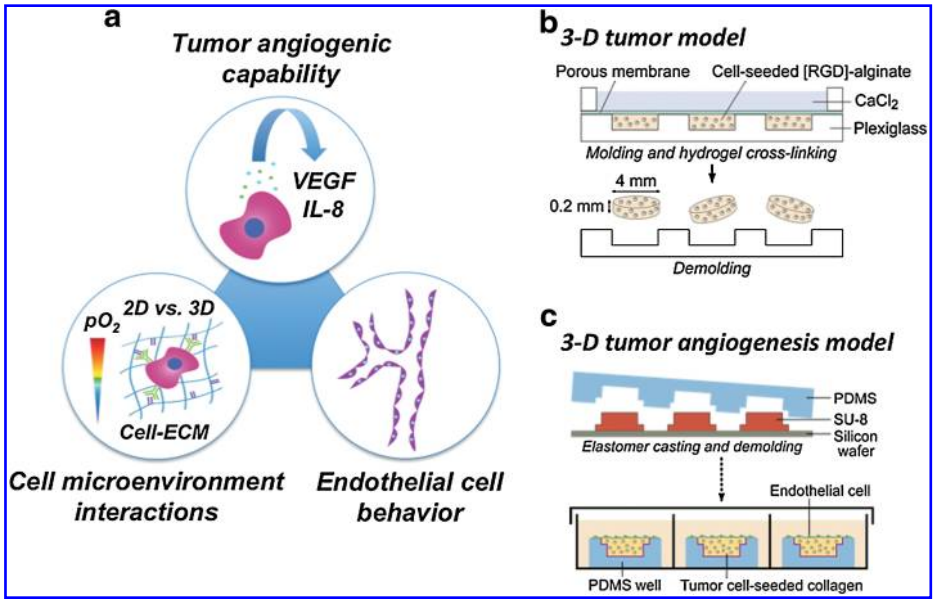

FIG. 1. Study design. (**a**) To study the pro-angiogenic capability of tumor cells in response to three-dimensional (3D) culture, oxygen (O_2) level, and cell–matrix interactions, oral squamous cell carcinoma (OSCC-3) was cultured within unmodified and RGD-modified alginate disks and vascular endothelial growth factor (VEGF) and interleukin-8 (IL-8) secretion was analyzed. Subsequently, the effects of tumor-secreted factors on endothelial cell behavior were determined using a new collagen-based 3D model of invasion. (**b**) Fabrication of OSCC-3-seeded alginate disks. Alginate solutions were mixed with cells, cast in a micromachined mold, and cross-linked with 60 mM $CaCl_2$. The resulting disks were removed from the mold and used for 3D culture. (**c**) Three-dimensional tumor angiogenesis models were fabricated by crosslinking of collagen/tumor cell mixtures within poly(dimethylsiloxane) (PDMS) molds that were microfabricated by conventional photolithography techniques. Human umbilical vein endothelial cells were then seeded on the top of these OSCC-3-seeded gels, followed by 3-day culture.

ethylenimine and 0.1% [v/v] glutaraldehyde to allow for the adhesion of collagen, (3) thermal cross-linking at 37°C for 30 min, and (4) top-seeding with HUVECs at 300 cell/mm^2 (Fig. 1c). Coculture was performed at ambient O_2 in Bio-Whittaker® medium 199 (M199; Lonza) with endothelial cell growth supplement (Millipore Co., Billerica, MA), 20% [v/v] fetal bovine serum, 1% [v/v] PS, 1% [v/v] L-ascorbic acid (50 µg/mL; Acros Organics, Morris Plains, NJ), and 0.16% [v/v] tetradecanoyl phorbol acetate (50 ng/mL; Cell Signaling Technology, Inc., Danvers, MA).

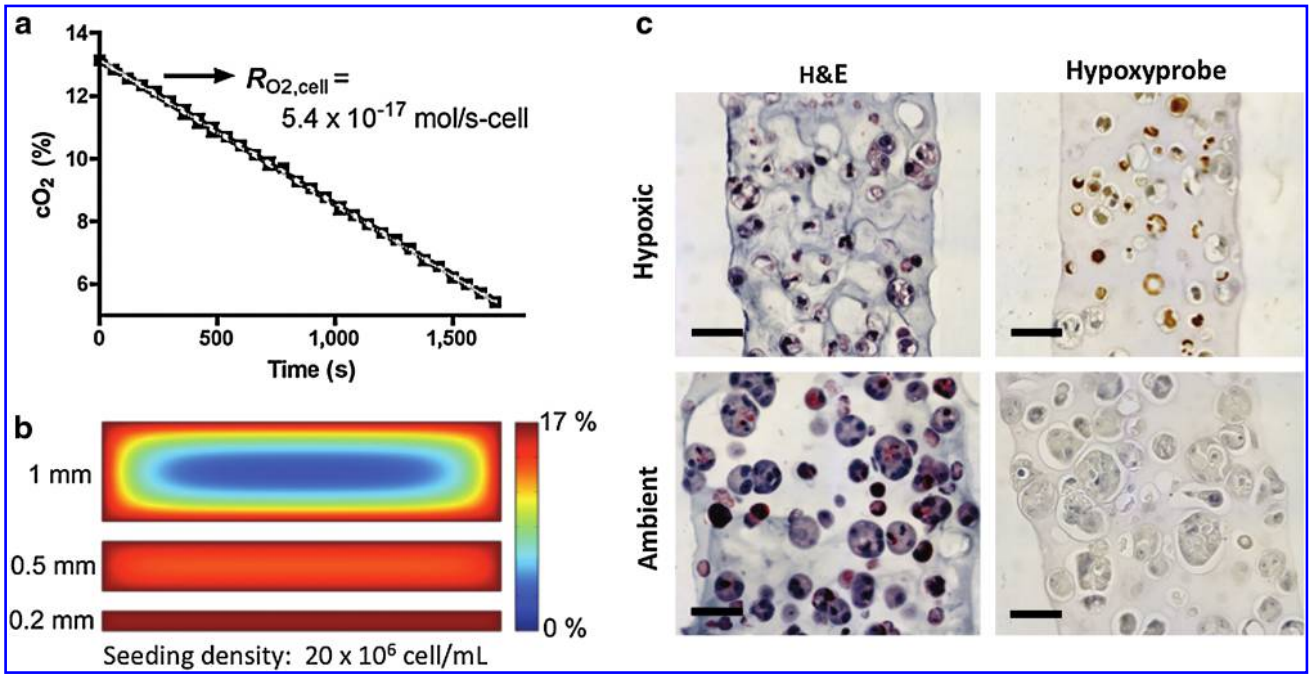

FIG. 2. Characterization of alginate-based 3D tumor models. (**a**) O_2 consumption of OSCC-3 cells seeded within 200-µm-thick alginate disks as quantified by a dissolved O_2 meter. (**b**) Cross-sectional O_2 levels of 3D tumor models at day 3 of culture as analyzed using finite element modeling for the measured OSCC-3 consumption rate, and for 200-, 500-, and 1000-µm-thick disks. (**c**) Histological characterization of alginate disks cultured for 6 days at hypoxic (1% O_2) and ambient ($18 \pm 1\%$ O_2) conditions. Hematoxylin and eosin staining indicates uniform cellularity of the developed 3D tumor models. Hypoxyprobe staining identifies hypoxic regions (hypoxic cells appear brown, with blue counterstaining) in cultures maintained at 1% O_2, whereas hypoxia was absent in systems cultured at ambient O_2. Scale bars represent 50 µm.

Confocal imaging

Confocal microscopy (LSM 510; Carl Zeiss, Inc.) was used to obtain z-stacks of 3D tumor angiogenesis models after 3 days of culture. Cell nuclei were stained with 4′,6-diamidino-2-phenylindole, actin was stained with Alexa Fluor® 568 phalloidin (Invitrogen Co.), and HUVECs were stained with mouse anti-human CD31 (BD Biosciences, San Jose, CA) and Alexa Fluor 488 goat anti-mouse IgG (Invitrogen Co.). Images were viewed and analyzed with ImageJ or LSM Image Browser (www.zeiss.com).

Statistical analysis

Statistical significance between conditions was assessed by Student's *t*-tests. In all figures, data are presented as mean ± standard deviation for one representative experiment. Significance between conditions is denoted as $*p < 0.05$, $**p < 0.01$, and $***p < 0.001$. At least two independent experiments were performed for each condition for verification of the emphasized trends. For protein and DNA values, individual measurements were taken on three separate samples for each condition. For the transwell migration analysis, 10 random images were counted and averaged per well, for three wells, for each condition. For invasion analysis, three random z-stacks were counted and averaged per scaffold, for three scaffolds, for each condition.

Results

Development and characterization of 3D tumor models with uniform O_2 distribution

To investigate the individual contributions of culture dimensionality and O_2 concentration on the angiogenic capability of tumor cells, we engineered 3D tumor models comprised of OSCC-3-seeded 200-μm-thick alginate disks (Fig. 1b). Cellular O_2 consumption was similar between OSCC-3 cultured in alginate ($R_{O_2,\text{cell}} = 5.4 \pm 0.2 \times 10^{-17}$ mol/(s·cell;) Fig. 2a), and those measured in suspension ($R_{O_2,\text{cell}} = 4.8 \pm 0.5 \times 10^{-17}$ mol/s-cell), confirming that neither encapsulation within alginate nor mechanical effects mediated by stirring affected the metabolic activity of these cells. Further, these rates were similar to the O_2 consumption rate reported for other tumor cells.[29,30] Finite element modeling of the steady-state O_2 distribution within the engineered tumors (cell density, measured O_2 consumption, and a reported O_2 diffusion value were used as inputs) indicated uniformity of O_2 levels within the engineered 200-μm-thick tumor models (central and peripheral oxygen partial pressure [pO_2] values differed by <2% for the initial seeding density [data not shown], and <4% after proliferation by a factor of three), whereas significant nonuniformity was predicted for tumor models ≥500 μm in thickness (>25% difference between central and peripheral pO_2 values at the initial seeding density for a 1-mm-thick scaffold, and 85% central depletion with proliferation by a factor of three) (Fig. 2b).

Histological analysis of 3D cultured tumor cells verified our ability to control cellularity and O_2 distribution in our systems. Hematoxylin and eosin staining indicated uniform cell distribution within both ambient and hypoxic 3D cultures, and that cell numbers were markedly enhanced in the tumor models exposed to ambient O_2 (Fig. 2c). Quantification of total DNA content confirmed that 3D cultured tumor cells proliferated significantly more at ambient O_2 than at hypoxia (increase in cell number at day 6 relative to day 0 was typically two- to threefold greater for ambient culture). Hypoxyprobe staining further confirmed uniform distribution of hypoxia for the 1% O_2 culture condition, whereas no staining was detected for the ambient culture (Fig. 2c). Tumor models cultured under ambient O_2 appeared to be thicker (closer to 250 μm) than their hypoxic counterparts after 6 days of culture, which could be a result of the enhanced proliferation and resulting disk swelling.

Secretion of pro-angiogenic factors in O_2-controlled 3D tumor models

To assess whether changes in global pO_2 affect the pro-angiogenic capability of OSCC-3 in 2D and 3D cultures, we measured secreted VEGF and IL-8 in the conditioned medium. Three-dimensional cultures of OSCC-3 exhibited a significant increase in VEGF and IL-8 secretion compared to 2D cultures for both ambient and hypoxic conditions (Fig. 3a). However, IL-8 was much more dramatically increased by 3D culture (20-fold for hypoxic and 116-fold for ambient culture) as compared to VEGF (fourfold for hypoxic and sevenfold for ambient culture) (Fig. 3a). Basic fibroblast growth factor was not the focus of these studies due to its low secretion levels. Consistent with previous results, hypoxia upregulated VEGF secretion in both 2D and 3D culture.[3,11] Interestingly, hypoxia increased IL-8 secretion in 2D culture (ambient: 0.022 ± 0.003 pg/ng DNA; hypoxic: 0.044 ± 0.003 pg/ng DNA),[11] but resulted in a threefold downregulation of IL-8 in 3D. These differences were due to changes in factor secretion rather than altered sequestration within the alginate matrix, as the measured amount of scaffold-sequestered VEGF and IL-8 was minimal under all tested conditions (data not shown). Collectively, these data indicate that hypoxia is a major regulator of VEGF in both 2D and 3D culture; however, other microenvironmental cues inherent to the 3D culture context, but lacking in conventional monolayer culture, appear to drive the upregulation of IL-8.

O_2-dependent changes in cell–ECM interactions alter secretion of angiogenic factors

To resolve the effects of hypoxia and 3D cell–ECM interactions on angiogenic factor secretion, we developed 3D tumor models using alginate hydrogels that were covalently modified with RGD-adhesion peptides to mimic fibronectin-mediated integrin engagement.[12] Subsequently, we compared VEGF and IL-8 secretion within nonmodified and RGD-modified alginate scaffolds maintained under ambient O_2 and hypoxia. Our results indicate important qualitative differences in angiogenic factor regulation by O_2 and cell–ECM interactions. While 3D cell–ECM interactions upregulate IL-8 secretion under both ambient and hypoxic culture conditions, IL-8 secretion is highest in the presence of the additive effects of ambient O_2 culture and 3D integrin engagement (Fig. 3b, right panel). In contrast, VEGF secretion is only moderately affected by 3D integrin engagement under ambient conditions, and unaffected in hypoxic cultures (Fig. 3b, left panel). Similar trends in VEGF and IL-8 secretion were detected when OSCC-3 cells were cultured in collagen scaffolds (Supplemental Fig. S2, available online at www.liebertonline.com/ten). As collagen also allows for

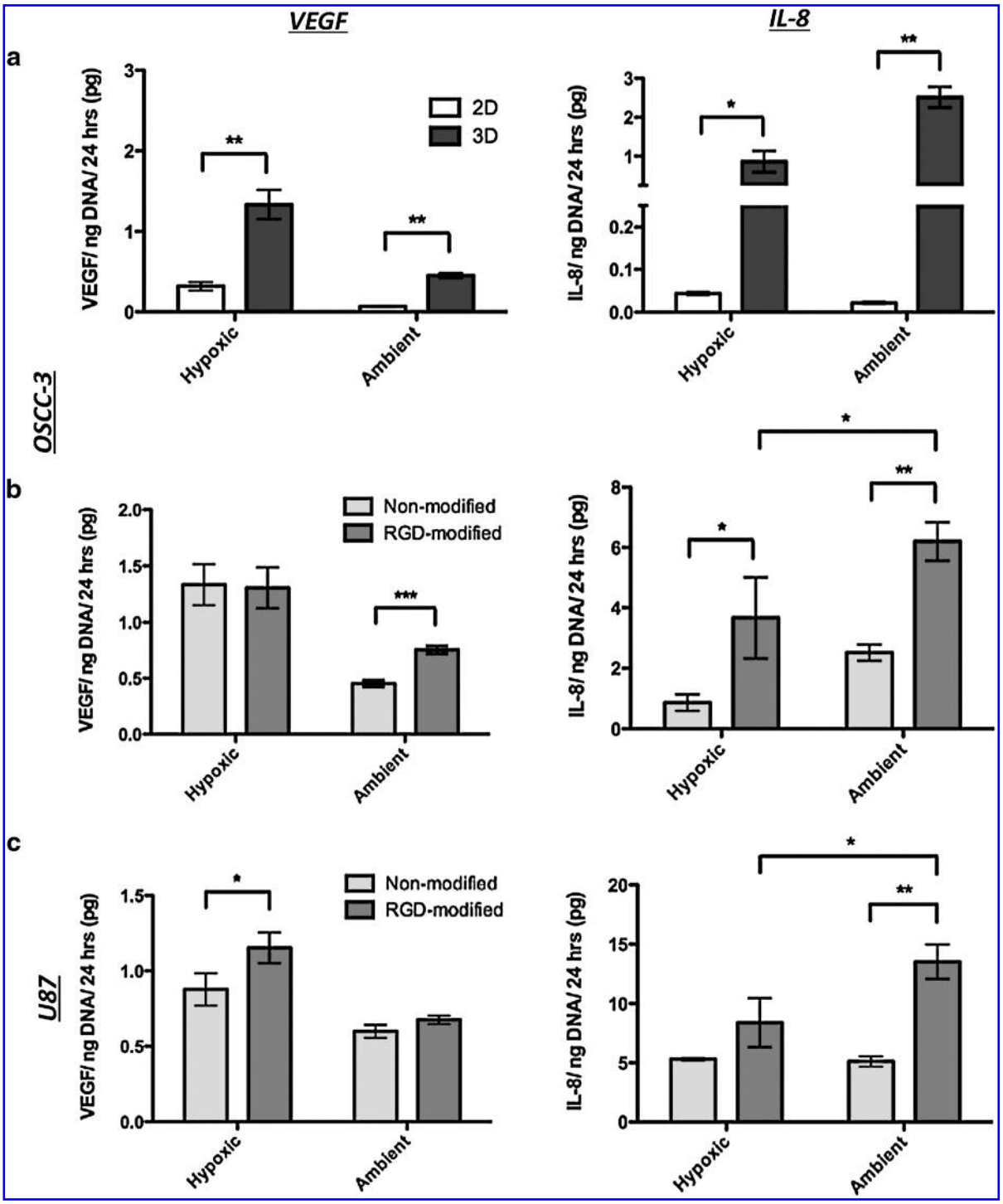

FIG. 3. Angiogenic factor secretion. (**a**) Effect of culture dimensionality (two-dimensional monolayer culture vs. 3D alginate culture) on VEGF and IL-8 secretion by OSCC-3 cells in response to hypoxia and ambient O_2 as measured by ELISA of the conditioned medium and normalization to DNA content. (**b**) Effect of 3D cell–extracellular matrix interactions on VEGF and IL-8 secretion by OSCC-3 cells in response to hypoxia and ambient O_2. To prevent and enable 3D integrin engagement, tumor cells were cultured within nonmodified or RGD-modified alginate disks, respectively. The conditioned medium was analyzed as described above. (**c**) Effect of 3D cell–extracellular matrix interactions on VEGF and IL-8 secretion by U87 cells in response to hypoxia and ambient O_2. All 3D medium samples were analyzed after 3 days of culture, whereas two-dimensional medium samples were measured after 2 days to prevent formation of 3D cell aggregates. ($^*p < 0.05$, $^{**}p < 0.01$, and $^{***}p < 0.001$).

integrin engagement, these results underline the importance of cell–ECM interactions in modulating the pro-angiogenic activity of OSCC-3, specifically with regard to IL-8 production.

To confirm the relevance of our findings with a second cell type, we analyzed the regulatory effects of O_2 and integrin engagement on VEGF and IL-8 secretion by U87 glioblastoma. In these cells VEGF was primarily regulated by hypoxia, and only affected by cell–ECM interactions under hypoxic conditions (Fig. 3c, left panel). In contrast, IL-8 was increased by integrin engagement independent of O_2, and was secreted most in ambient RGD-alginate cultures (Fig. 3c, right panel). Together, VEGF and IL-8 secretion by OSCC-3 and U87 is similarly regulated by the O_2 and ECM environment, underlining the significance of our findings.

Changes in 3D cell proliferation may induce altered integrin engagement due to sequestration of ECM molecules in tumor cell aggregates.[31,32] As OSCC-3 cells proliferated two to three times faster in ambient relative to hypoxic cultures, we tested this possible relationship. Inhibition of OSCC-3 proliferation by mitomycin-C reduced IL-8 and VEGF secretions in ambient 3D alginate cultures (VEGF: twofold decrease; IL-8: threefold decrease; data not shown). These data indicate that O_2-dependent changes in proliferation play a significant role in guiding angiogenic factor secretion, and it is possible that differential ECM deposition may be involved in this effect.

O_2-dependent changes in angiogenic signaling regulate angiogenesis

To explore the implications of IL-8 upregulation in response to ambient 3D culture conditions, we performed a transwell assay in which we measured HUVEC migration in response to the tumor-conditioned medium in the absence and presence of IL-8-function blocking antibody. The tumor-conditioned medium collected from alginate-based 3D OSCC-3 models maintained under ambient O_2 significantly ($p < 0.05$) elevated HUVEC migration relative to the control medium, and neutralization of IL-8 blocked this effect (control medium: 72 ± 11; tumor medium: 109 ± 12; tumor medium + anti-IL-8 Ab: 87 ± 6 migrations/mm^2). These results indicate that IL-8 upregulation in response to the combined effects of ambient O_2 and tumor dimensionality plays an important role in regulating the migratory capacity of endothelial cells during tumor angiogenesis.

Although transwell studies provide important tools to study endothelial cell behavior in culture, they lack the 3D cell–microenvironment interactions that regulate invasion angiogenesis *in vivo*. To overcome these limitations we developed a 3D coculture system to study tumor angiogenesis *in vitro*. This microfabricated model consisted of a tumor-cell-incorporating remodelable collagen scaffold that was coated with an endothelial cell monolayer (Fig. 1c). O_2 concentrations within this 3D tumor angiogenesis model can be adjusted by varying the seeding density of the tumor cells and the height of the PDMS mold used to cast the collagen gels. Specifically, scaffolds containing either 5×10^6 or 20×10^6 OSCC-3/mL (or no tumor cells as a control) were fabricated and thermally cross-linked in PDMS microcarriers of 90 and 400 μm depth. Mathematical modeling (assuming proliferation by a factor of three of the initial seeding density over the course of the 3-day culture) of O_2 distribution within these microwell cultures confirmed that 90-μm-thick cultures developed homogenous (>97% uniformity) ambient O_2 concentrations at both cell densities (Fig. 4a). However, O_2 was reduced to < 50% of the ambient O_2 concentration at the base of the 400-μm-thick higher seeding density culture, providing a heterogeneous O_2 environment characteristic of tumors *in vivo* (Fig. 4a).

Angiogenic response to these conditions was analyzed by quantifying HUVEC invasion into the underlying tumor matrix (Fig. 4b, c). HUVECs readily invaded blank collagen scaffolds and sparse 3D tumor cell cultures devoid of hypoxia (i.e., seeding density: 5×10^6 cells/mL; thickness: 90 μm), but invasion was dramatically increased with enhanced tumor cell density (i.e., 20×10^6 cells/mL; thickness: 90 μm) (Fig. 4c). We hypothesized that this difference could be related to the cell-number-dependent increase of IL-8 under ambient conditions rather than the increase in VEGF, as HUVEC invasion into thick cultures with heterogeneous O_2 distribution (i.e., seeding density: 20×10^6 cells/mL; thickness: 400 μm) was significantly reduced. To test our hypothesis, we measured IL-8 secretion in the different culture models, which confirmed that increased endothelial cell invasion correlated with IL-8 upregulation (data not shown). These novel 3D tumor models have the potential to transform current studies of tumor angiogenesis by enabling precise control over the 3D cell–microenvironment interactions that may contribute to tumor angiogenesis. Further qualitative and quantitative characterization of these culture systems will be necessary to resolve the contributions of IL-8 upregulation in response to O_2-dependent 3D culture conditions.

Discussion

We have engineered 3D microscale tumor models to experimentally isolate the effects of tumor O_2 tension, culture dimensionality, and cell–ECM interactions on the angiogenic capability of OSCC-3. Hypoxia enhanced VEGF secretion in both 2D and 3D cultures. IL-8 was enhanced by hypoxia in 2D culture, whereas an opposite trend was noted for OSCC-3 IL-8 secretion in 3D culture. While cell–ECM interactions increased IL-8 secretion independent of O_2, these conditions modulated VEGF secretion only under ambient culture conditions. Similar trends were observed for OSCC-3 cultured in collagen I and U87 cells maintained in alginate-based systems, thereby underlining the significance of our findings. Using 2D migration assays and a novel 3D tumor angiogenesis model, we demonstrated that the resulting angiogenic signaling affects endothelial cell behavior.

These studies are broadly relevant to our understanding of tumor angiogenesis as they may help to explain the differential amounts and spatial distribution of VEGF and IL-8 in tumors *in vivo*. Although small tumors secrete more IL-8 than large tumors, more VEGF is predominant in large tumors.[33] Further, IL-8 is preferentially localized in the tumor periphery, whereas VEGF is primarily associated with the center of tumors.[33] Our results suggest that these spatial differences may be due to their primary mechanisms of regulation: hypoxia (i.e., the main regulator of VEGF) is increased in large tumors and predominantly present in the center, whereas the relative amount of O_2 and 3D cell–ECM interactions (i.e., a primary regulator of IL-8) is enhanced in small tumors and the periphery of larger tumors.

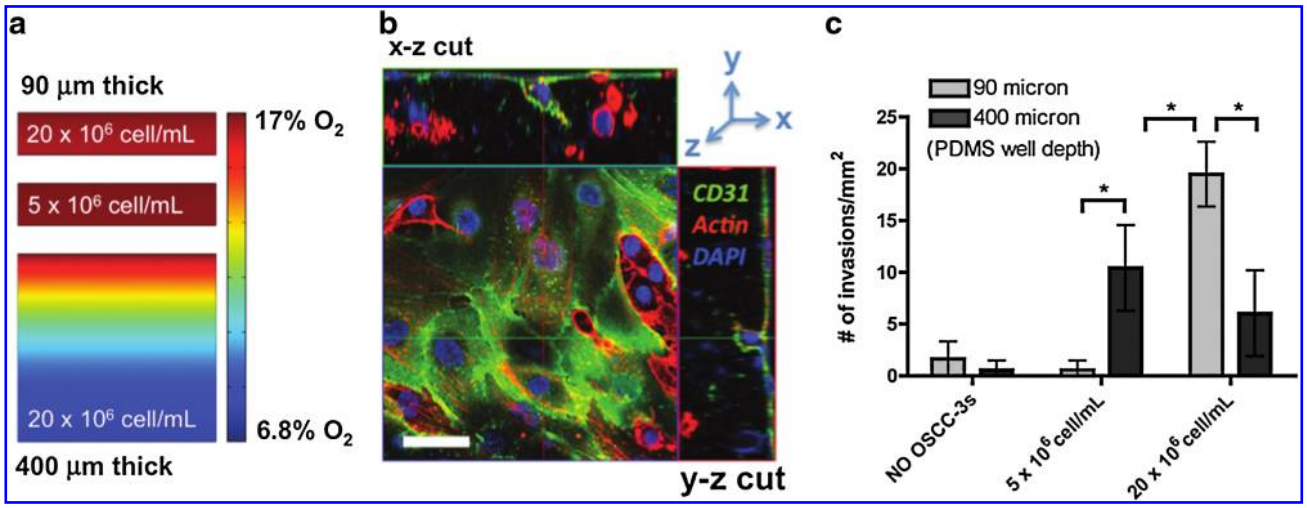

FIG. 4. Three-dimensional tumor angiogenesis model. (**a**) Finite element modeling of O_2 distribution in tumor-angiogenesis models of varying cell density and scaffold thickness (90 and 400 μm) to mimic intratumoral spatial variations in O_2 levels. Indicated cell numbers (5×10^6 and 20×10^6 cells/mL) represent initial seeding densities, and finite element models account for proliferation by a factor of three after 3 days of culture. (**b**) Analysis of endothelial cell invasion was performed by confocal imaging subsequent to staining for cell nuclei (blue), actin (red), and the endothelial cell marker CD31 (green). Scale bar represents 50 μm. (**c**) Number of invading human umbilical vein endothelial cells/mm^2 ($\geq$10 μm in depth) quantified for three initial OSCC-3 seeding densities (0, 5×10^6, and 20×10^6 cells/mL) and two collagen scaffold thicknesses (90 and 400 μm) at day 3 of culture ($^*p < 0.05$).

We have previously shown that proliferation of OSCC-3 in 3D culture leads to upregulation of fibronectin relative to monolayer culture,[11] and that the resulting 3D integrin engagement enhances IL-8, but not VEGF secretion.[12] By experimentally isolating O_2, culture dimensionality, and cell–ECM interactions, we now present evidence that supports a model of O_2-dependent differences in the regulation of VEGF and IL-8 secretion by 3D integrin engagement. While VEGF secretion is only modestly regulated by 3D cell–ECM interactions, at ambient culture for OSCC-3 and hypoxic culture for U87s, IL-8 secretion is significantly increased by these interactions regardless of the O_2 environment, for both cell types. This difference may be related to differences in integrin signaling under hypoxic culture conditions that may activate hypoxia inducible factor-1α (HIF-1α), a transcription factor that regulates VEGF, but not IL-8 expression.[34,35]

To assess the potential impact of O_2-dependent IL-8 upregulation, we developed coculture models that mimicked paracrine signaling between tumor and endothelial cells. Transwell migration experiments using the conditioned medium from ambient OSCC-3 cultures validated that IL-8 upregulation increases the migratory capacity of endothelial cells.[36,37] However, migratory capacity does not encompass the full angiogenic behavior of endothelial cells, and does not necessarily correlate to a cell's contribution to invasion angiogenesis. To more appropriately test tumor angiogenesis as affected by 3D cultured tumor cells *in vitro*, we have developed a system that may have broad utility as an invasion assay. In this system the scaffold can be remodeled by both tumor and endothelial cells, as is the case *in vivo*, and the combined effects of O_2, soluble factors, and dimensionality of cell–microenvironment interactions can be studied under pathologically relevant conditions.

While our studies focused on defining the distinct roles of O_2 and 3D cell–ECM interactions in modulating the angiogenic potential of tumor cells, the developed model systems have broad utility for testing multiple key questions still unresolved in the field of tumor angiogenesis. For example, O_2-dependent changes in cell proliferation may alter cell–cell interactions via direct cell–cell contact and altered paracrine signaling.[38,39] By covalent coupling of cell–cell adhesion molecules (e.g., cadherins) to alginate or utilization of alginate-based matrices to recreate biologically inspired delivery profiles of soluble factors (e.g., gradients), it may become possible to study the role of these cues under defined O_2 and 3D culture conditions. Finally, while ambient O_2 is commonly employed in cell culture work, physiological tissue O_2 levels are significantly lower.[40,41] Future studies with these 3D culture systems will allow us to define the quantitative range of O_2 concentration profiles that may modulate tumor angiogenesis.

In summary, we have developed broadly applicable 3D tumor and tumor angiogenesis models by integrating engineering tools and cancer biology. These systems allow studies of cancer biology under pathologically relevant culture conditions *in vitro*. Future applications may lead to an improved understanding of tumor angiogenesis that has the potential to improve current antiangiogenic treatment regimes and ultimately the clinical prognosis of cancer patients.

Acknowledgments

We acknowledge funding from the Cornell Nanobiotechnology Center (supported by the STC Program of the National Science Foundation under Agreement No. ECS-9876771), the Beckman Foundation, NYSTAR, the Morgan Fund for Tissue Engineering, and National Institutes of Health (RC1 CA146065 and 1U54 CA143876-01). We would also like to thank Guen Bradbury and Brian Kwee for their general assistance with experiments and helpful discussions.

Disclosure Statement

No competing financial interests exist.

References

1. Hanahan, D., and Weinberg, R.A. The hallmarks of cancer. Cell **100,** 57, 2000.
2. Bergers, G., and Benjamin, L.E. Tumorigenesis and the angiogenic switch. Nat Rev Cancer **3,** 401, 2003.
3. Harris, A.L. Hypoxia—a key regulatory factor in tumour growth. Nat Rev Cancer **2,** 38, 2002.
4. Forsythe, J.A., Jiang, B.H., Iyer, N.V., Agani, F., Leung, S.W., Koos, R.D., and Semenza, G.L. Activation of vascular endothelial growth factor gene transcription by hypoxia-inducible factor 1. Mol Cell Biol **16,** 4604, 1996.
5. Maxwell, P.H., Dachs, G.U., Gleadle, J.M., Nicholls, L.G., Harris, A.L., Stratford, I.J., Hankinson, O., Pugh, C.W., and Ratcliffe, P.J. Hypoxia-inducible factor-1 modulates gene expression in solid tumors and influences both angiogenesis and tumor growth. PNAS **94,** 8104, 1997.
6. Folkman, J., Bach, M., Rowe, J.W., Davidoff, F., Lambert, P., Hirsch, C., Goldberg, A., Hiatt, H.H., Glass, J., and Henshaw, E. Tumor angiogenesis—therapeutic implications. N Engl J Med **285,** 1182, 1971.
7. Kerbel, R.S. Molecular origins of cancer: tumor angiogenesis. N Engl J Med **358,** 2039, 2008.
8. Folkman, J., and Klagsbrun, M. Angiogenic factors. Science **235,** 442, 1987.
9. Bissell, M.J., and Radisky, D. Putting tumours in context. Nat Rev Cancer **1,** 46, 2001.
10. Ingber, D.E. Can cancer be reversed by engineering the tumor microenvironment? Semin Cancer Biol **18,** 356, 2008.
11. Fischbach, C., Chen, R., Matsumoto, T., Schmelzle, T., Brugge, J.S., Polverini, P.J., and Mooney, D.J. Engineering tumors with 3D scaffolds. Nat Methods **4,** 855, 2007.
12. Fischbach, C., Kong, H.J., Hsiong, S.X., Evangelista, M.B., Yuen, W., and Mooney, D.J. Cancer cell angiogenic capability is regulated by 3D culture and integrin engagement. Proc Natl Acad Sci USA **106,** 399, 2009.
13. Jain, R.K. Normalization of tumor vasculature: an emerging concept in antiangiogenic therapy. Science **307,** 58, 2005.
14. Mizukami, Y., Jo, W.S., Duerr, E.M., Gala, M., Li, J.N., Zhang, X.B., Zimmer, M.A., Iliopoulos, O., Zukerberg, L.R., Kohgo, Y., Lynch, M.P., Rueda, B.R., and Chung, D.C. Induction of interleukin-8 preserves the angiogenic response in HIF-1 alpha-deficient colon cancer cells. Nat Med **11,** 992, 2005.
15. Casanovas, O., Hicklin, D.J., Bergers, G., and Hanahan, D. Drug resistance by evasion of antiangiogenic targeting of VEGF signaling in late-stage pancreatic islet tumors. Cancer Cell **8,** 299, 2005.
16. Lal, A., Peters, H., St. Croix, B., Haroon, Z.A., Dewhirst, M.W., Strausberg, R.L., Kaanders, J., van der Kogel, A.J., and Riggins, G.J. Transcriptional response to hypoxia in human tumors. J Natl Cancer Inst **93,** 1337, 2001.
17. Richard, D.E., Berra, E., and Pouyssegur, J. Angiogenesis: how a tumor adapts to hypoxia. Biochem Biophys Res Commun **266,** 718, 1999.
18. Zhong, H., De Marzo, A.M., Laughner, E., Lim, M., Hilton, D.A., Zagzag, D., Buechler, P., Isaacs, W.B., Semenza, G.L., and Simons, J.W. Overexpression of hypoxia-inducible factor 1 alpha in common human cancers and their metastases. Cancer Res **59,** 5830, 1999.
19. Semenza, G.L. Involvement of hypoxia-inducible factor 1 in human cancer. Intern Med **41,** 79, 2002.
20. Pampaloni, F., Reynaud, E.G., and Stelzer, E.H.K. The third dimension bridges the gap between cell culture and live tissue. Nat Rev Mol Cell Biol **8,** 839, 2007.
21. Albrecht, D.R., Underhill, G.H., Wassermann, T.B., Sah, R.L., and Bhatia, S.N. Probing the role of multicellular organization in three-dimensional microenvironments. Nat Methods **3,** 369, 2006.
22. Lee, G.Y., Kenny, P.A., Lee, E.H., and Bissell, M.J. Three-dimensional culture models of normal and malignant breast epithelial cells. Nat Methods **4,** 359, 2007.
23. Choi, N.W., Cabodi, M., Held, B., Gleghorn, J.P., Bonassar, L.J., and Stroock, A.D. Microfluidic scaffolds for tissue engineering. Nat Mater **6,** 908, 2007.
24. Heywood, H.K., Sembi, P.K., Lee, D.A., and Bader, D.L. Cellular utilization determines viability and matrix distribution profiles in chondrocyte-seeded alginate constructs. Tissue Eng **10,** 1467, 2004.
25. Cheema, U., Brown, R.A., Alp, B., and MacRobert, A.J. Spatially defined oxygen gradients and vascular endothelial growth factor expression in an engineered 3D cell model. Cell Mol Life Sci **65,** 177, 2008.
26. Rowley, J.A., Madlambayan, G., and Mooney, D.J. Alginate hydrogels as synthetic extracellular matrix materials. Biomaterials **20,** 45, 1999.
27. Fursov, N., Cong, M., Federici, M., Platchek, M., Haytko, P., Tacke, R., Livelli, T., and Zhong, Z. Improving consistency of cell-based assays by using division-arrested cells. Assay Drug Dev Technol **3,** 7, 2005.
28. Spaeth, E.E., and Friedlander, S.K. Diffusion of oxygen carbon dioxide and inert gas in flowing blood. Biophys J **7,** 827, 1967.
29. Ruffieux, P.A., von Stockar, U., and Marison, I.W. Measurement of volumetric (OUR) and determination of specific (qO(2)) oxygen uptake rates in animal cell cultures. J Biotechnol **63,** 85, 1998.
30. Muellerklieser, W., Zander, R., and Vaupel, P. A new photometric-method for oxygen-consumption measurements in cell-suspensions. J Appl Physiol **61,** 449, 1986.
31. Zhang, Y., Lu, H., Dazin, P., and Kapila, Y. Squamous cell carcinoma cell aggregates escape suspension-induced, p53-mediated anoikis—Fibronectin and integrin alpha(v) mediate survival signals through focal adhesion kinase. J Biol Chem **279,** 48342, 2004.
32. Simpson-Haidaris, P.J., and Rybarczyk, B. Tumors and fibrinogen—the role of fibrinogen as an extracellular matrix protein. In: Nieuwenhuizen, W., Mosesson, M.W., and De-Maat, M.P.M., eds. Proceedings paper from Annals of the New York Academy of Sciences, vol. 936. New York: New York Academy of Sciences, 2001, pp. 406–425.
33. Kumar, R., Kuniyasu, H., Bucana, C.D., Wilson, M.R., and Fidler, I.J. Spatial and temporal expression of angiogenic molecules during tumor growth and progression. Oncol Res **10,** 301, 1998.
34. Skuli, N., Monferran, S., Delmas, C., Favre, G., Bonnet, J., Toulas, C., and Moyal, E.C.J. Alpha(v)beta(3)/alpha(v) beta(5) integrins-FAK-RhoB: a novel pathway for hypoxia regulation in glioblastoma. Cancer Res **69,** 3308, 2009.
35. Xie, K.P. Interleukin-8 and human cancer biology. Cytokine Growth Factor Rev **12,** 375, 2001.
36. Waugh, D.J.J., and Wilson, C. The interleukin-8 pathway in cancer. Clin Cancer Res **14,** 6735, 2008.
37. Yuan, A., Chen, J.J.W., Yao, P.L., and Yang, P.C. The role of interleukin-8 in cancer cells and microenvironment interaction. Front Biosci **10,** 853, 2005.

38. Tan, C.P., Seo, B.R., Brooks, D.J., Chandler, E.M., Craighead, H.G., and Fischbach, C. Parylene peel-off arrays to probe the role of cell-cell interactions in tumour angiogenesis. Integr Biol **1,** 587, 2009.
39. Cavallaro, U., Liebner, S., and Dejana, E. Endothelial cadherins and tumor angiogenesis. Exp Cell Res **312,** 659, 2006.
40. Simon, M.C., and Keith, B. The role of oxygen availability in embryonic development and stem cell function. Nat Rev Mol Cell Biol **9,** 285, 2008.
41. Hockel, M., and Vaupel, P. Tumor hypoxia: definitions and current clinical, biologic, and molecular aspects. J Natl Cancer Inst **93,** 266, 2001.

Address correspondence to:
Claudia Fischbach, Ph.D.
Department of Biomedical Engineering
Cornell University
157 Weill Hall
Ithaca, NY 14853

E-mail: cf99@cornell.edu

Received: October 7, 2009
Accepted: March 8, 2010
Online Publication Date: April 9, 2010